THE JOURNAL OF BIOLOGICAL CHEMISTRY VOL. 285, NO. 26, pp. 19854–19864, June 25, 2010

Calcium-sensing Receptor Biosynthesis Includes a Cotranslational Conformational Checkpoint and Endoplasmic Reticulum Retention*

Received for publication, March 18, 2010, and in revised form, April 19, 2010 Published, JBC Papers in Press, April 26, 2010, DOI 10.1074/jbc.M110.124792

Alice Cavanaugh, Jennifer McKenna, Ann Stepanchick, and Gerda E. Breitwieser[1]

From the Weis Center for Research, Geisinger Clinic, Danville, Pennsylvania 17822

Metabolic labeling with [^{35}S]cysteine was used to characterize early events in CaSR biosynthesis. [^{35}S]CaSR is relatively stable (half-life ~8 h), but maturation to the final glycosylated form is slow and incomplete. Incorporation of [^{35}S]cysteine is linear over 60 min, and the rate of [^{35}S]CaSR biosynthesis is significantly increased by the membrane-permeant allosteric agonist NPS R-568, which acts as a cotranslational pharmacochaperone. The [^{35}S]CaSR biosynthetic rate also varies as a function of conformational bias induced by loss- or gain-of-function mutations. In contrast, [^{35}S]CaSR maturation to the plasma membrane was not significantly altered by exposure to the pharmacochaperone NPS R-568, the allosteric agonist neomycin, or the orthosteric agonist Ca^{2+} (0.5 or 5 mM), suggesting that CaSR does not control its own release from the endoplasmic reticulum. A CaSR chimera containing the mGluR1α carboxyl terminus matures completely (half-time of ~8 h) and without a lag period, as does the truncation mutant CaSRΔ868 (half-time of ~16 h). CaSRΔ898 exhibits maturation comparable with full-length CaSR, suggesting that the CaSR carboxyl terminus between residues Thr^{868} and Arg^{898} limits maturation. Overall, these results suggest that CaSR is subject to cotranslational quality control, which includes a pharmacochaperone-sensitive conformational checkpoint. The CaSR carboxyl terminus is the chief determinant of intracellular retention of a significant fraction of total CaSR. Intracellular CaSR may reflect a rapidly mobilizable "storage form" of CaSR and/or may subserve distinct intracellular signaling roles that are sensitive to signaling-dependent changes in endoplasmic reticulum Ca^{2+} and/or glutathione.

Biosynthesis of G protein-coupled receptors (GPCRs)[2] is complex and requires successful navigation of multiple quality control checkpoints prior to release from the endoplasmic reticulum (ER) and transport to the plasma membrane (reviewed in Refs. 1 and 2). GPCRs are subject to cotranslational glycosylation at one or more asparagines, and many are stabilized by a disulfide bond between cysteines in extracellular loops 1 and 2 (2–4). The arrangement of helices within the monomer is also subject to stringent quality control and is prone to failure (reviewed in Refs. 3 and 4). It has been suggested that the conformational flexibility required for agonist-mediated activation predisposes GPCRs to folding difficulties and low efficiency in biosynthesis (3, 5). Rescue of misfolded GPCRs can be achieved by block of proteasomal degradation, probably providing time for additional folding attempts (*e.g.* see Refs. 6 and 7). Alternatively, folding of both WT and mutant GPCRs, including V2 vasopressin receptors (8, 9), κ- and δ-opioid receptors (10–12), and gonadotropin-releasing hormone receptors (13, 14), can be facilitated by membrane-permeant agonists or antagonists acting as pharmacochaperones to stabilize helix packing by binding in the transmembrane heptahelical domain.

CaSR, a Family C/3 GPCR, has several unique structural features that further complicate biosynthesis. The large extracellular domain (ECD), which binds agonist and some allosteric modulators, contains 11 putative glycosylation sites (15) and is stabilized by multiple intramolecular disulfide bonds (16). CaSR is an obligate dimer, with an intermolecular disulfide bond formed at Lobe I residues Cys^{129}/Cys^{131} plus hydrophobic interactions within the ECD (17, 18). Both the ECD and heptahelical domains of CaSR contain allosteric sites that modulate responses elicited by Ca^{2+} binding at the orthosteric site of the ECD (reviewed in Refs. 19 and 20). CaSR is subject to endoplasmic reticulum-associated degradation (ERAD) via the E3 ligase dorfin as part of a multistep quality control process during the early stages of CaSR biosynthesis (7, 21).

Calcium-handling diseases result from mutations in CaSR; loss-of-function mutations cause familial hypocalciuric hypercalcemia or neonatal severe primary hyperparathyroidism, and gain-of-function mutations cause autosomal dominant hypocalcemia (Bartters syndrome type V) (21). Many CaSR loss-of-function mutations interfere with proper trafficking of CaSR through the secretory pathway and can be rescued in functional form to the plasma membrane by overnight treatment with the allosteric agonist NPS R-568 (21, 22). Conversely, some gain-of-function mutants are resistant to ERAD, but their degradation in the ER can be promoted by the allosteric antagonist NPS 2143 (21). CaSR biosynthetic quality control may therefore include a unique conformation-sensitive

* This work was supported, in whole or in part, by National Institutes of Health Grant R01 GM077563. This work was also supported by funds from the Geisinger Clinic (to G. E. B.).

[1] To whom correspondence should be addressed: Weis Center for Research, Geisinger Clinic, 100 N. Academy Ave., Danville, PA 17822-2604. Fax: 570-271-5886; E-mail: gebreitwieser@geisinger.edu.

[2] The abbreviations used are: GPCR, G protein-coupled receptor; ER, endoplasmic reticulum; WT, wild type; ECD, extracellular domain; ERAD, endoplasmic reticulum-associated degradation; CT, carboxyl terminus; EGFP, enhanced green fluorescent protein; OK, opossum kidney; GAPDH, glyceraldehyde-3-phosphate dehydrogenase; ELISA, enzyme-linked immunosorbent assay; IP, immunoprecipitation; WB, Western blot; DMEM, Dulbecco's modified Eagle's medium.

checkpoint controlling total and plasma membrane expression of WT and mutant CaSRs (21).

Here we examine the very early events in CaSR biosynthesis by monitoring the appearance and maturation of [^{35}S]cysteine-labeled CaSR. Results indicate that [^{35}S]CaSR that accumulates during the pulse label period has undergone cotranslational quality control. CaSR therefore rapidly navigates both generic (glycosylation, disulfide bond shuffling) and specific (helix packing, conformational assessment) quality control checkpoints, and the pharmacochaperone NPS R-568 acts cotranslationally to stabilize [^{35}S]CaSR. CaSR dimers that successfully run the gauntlet enjoy prolonged stability in the ER until release to the Golgi and plasma membrane. Neither membrane-permeant (NPS R-568) nor membrane-impermeant (neomycin) allosteric agonists or Ca^{2+} are able to facilitate full [^{35}S]CaSR maturation, but truncation of the carboxyl terminus (CT) induces full [^{35}S]CaSR maturation. These results suggest that the CaSR CT is the chief determinant of both the rate of CaSR maturation through the secretory pathway and the subcellular localization of the net cellular complement of CaSR. Such control of the levels of both intracellular and plasma membrane CaSR suggests the exciting possibility of an intracellular signaling role(s) for CaSR.

MATERIALS AND METHODS

cDNA Constructs—All constructs in pEGFP-N1 were generated using PCR primer mutagenesis with *Pfu Ultra* polymerase (Stratagene) in the background of human CaSR containing an amino-terminal FLAG epitope immediately after the signal sequence (FLAG-CaSR) (23). Point mutations in the WT FLAG-CaSR background (E837I, A843E, and L849P) were generated as described previously (22). The CaSR/mGluR1α CT chimera was generated by incorporating a silent PvuI restriction site at the proposed junction in both CaSR and mGluR1α constructs, digesting each vector with PvuI, followed by ligation. The final CaSR/mGluR1α construct contains WT FLAG-CaSR through residue 869, followed by rat mGluR1α residues 849–1194, followed by EGFP. To rule out a contribution of EGFP to the observed maturation rate, FLAG-CaSR-EGFP (FLAG-CaSR fused after residue 1078 to EGFP) was used as the control. A stop codon was incorporated into FLAG-CaSR by PCR mutagenesis to generate CaSR truncations (CaSRΔ868, CaSRΔ880, CaSRΔ886, CaSRΔ898, CaSRΔ1024, and CaSRΔ1052). All constructs were confirmed by sequencing (Genewiz).

Cell Culture and [^{35}S]Cysteine Metabolic Labeling of CaSR—HEK293 and opossum kidney (OK) cells were obtained from ATCC and cultured as recommended in minimum Eagle's medium (Mediatech) supplemented with 10% fetal bovine serum and penicillin/streptomycin in 5% CO_2 and used within 25 passages. Cells were plated (10^6 cells/100-mm dish) and allowed to attach overnight before transfection. Each plate was transfected with 6 μg of FLAG-CaSR or FLAG-CaSR mutant cDNA plus 18 μl of Fugene HD (Roche Applied Science) for 24 h. Cells were starved for 30 min in normal Ca^{2+}-containing DMEM without cysteine or methionine (Invitrogen). Labeling was initiated by the addition of [^{35}S]cysteine (PerkinElmer Life Sciences; 1075 Ci/mmol) at a final concentration of 100 μCi/ml and methionine to a final concentration of 2.3 mM. Drug treatments were added as indicated for individual experiments, with control samples containing equivalent volumes of the solvent (DMSO). After labeling, plates were rinsed with phosphate-buffered saline, and medium was replaced with minimum Eagle's medium containing 10% fetal bovine serum. Labeled cells were lysed and processed for immunoprecipitation and Western blotting immediately or at variable chase times.

Immunoprecipitation and Western Blotting—Cells were lysed (5 mM EDTA, 0.5% Triton X-100, 10 mM iodoacetamide, plus Complete protease inhibitor tablet (Roche Applied Science) in phosphate-buffered saline) and cleared at 4 °C with Sepharose CL-2B (Sigma). Equal amounts of protein (micro-BCA protein assay, Pierce) were immunoprecipitated overnight with M2 anti-FLAG antibody (Sigma) plus anti-GAPDH monoclonal antibody (Abcam) and protein G-agarose (Invitrogen). Samples were eluted in SDS loading buffer containing 100 mM dithiothreitol, incubated at 22 °C for 30 min, run on 4–15% SDS-polyacrylamide gels (Criterion, Bio-Rad) and transferred onto nitrocellulose. [^{35}S]CaSR was detected on an Amersham Biosciences Storm 840 Imager, followed by processing of the blot for total protein. Blots were cut at the 75 kDa marker, and CaSR was detected on the upper portion with rabbit polyclonal anti-LRG antibody (1:2000; custom-generated by Genemed Synthesis, Inc. against LRG epitope residues 374–391), and the lower part of each blot was probed with rabbit polyclonal anti-GAPDH antibody (1:2000; Abcam). ECL anti-rabbit IgG, horseradish peroxidase-linked F(ab′)$_2$ fragment from donkey (GE Healthcare) was the secondary antibody. SuperSignal West Pico Chemiluminescence Substrate (Pierce) was used to visualize proteins to film, followed by scanning to computer and analysis with AlphaEaseFC version 4.0.0 (Alpha Innotech) or by direct chemiluminescence visualization on a FUJIFILM LAS-4000mini luminescent analyzer and processing with Image-Gauge version 3.0.

Data Analysis and Statistics—All experiments were repeated a minimum of 3–5 times (as indicated in individual figure legends). Immunoprecipitation of endogenous GAPDH was used as a loading control. Pixel intensities of [^{35}S]CaSR (obtained from Amersham Biosciences Storm Image, ImageQuant software) were divided by the pixel intensities of GAPDH (obtained on Western blot by FUJIFILM LAS-4000mini, Multi-Gauge software version 3.0). For rate of biosynthesis, data in individual experiments were normalized to the control condition at 15 min; multiple experiments were then averaged at each time point. Pulse-chase data were normalized to GAPDH intensities, and then the normalized abundance was determined at each time point as the percentage intensity of the form (140 or 160 kDa) relative to the total [^{35}S]CaSR intensity at that time point (140 plus 160 kDa bands). S.D. or S.E values were calculated with Microsoft Excel; significance was determined by Student's t test at $p < 0.05$.

ELISAs of CaSR Localization—HEK293 or OK cells were transfected with 1 μg of FLAG-CaSR or FLAG-CaSRΔ868 DNA plus FuGene HD (Roche Applied Science) in 6-well plates. After 24 h, each well was split into 16 wells of a 96-well poly-L-lysine-coated plate. At the times indicated, cells were washed with TBS-T (0.05 M Tris, pH 7.4, 0.15 M NaCl, 0.05%

Tween 20) and fixed (4% paraformaldehyde or MeOH) for 15 min on ice. Cells were blocked in TBS-T, 1% milk, followed by 60 min in TBS-T/monoclonal anti-FLAG-M2-horseradish peroxidase antibody (1:5000; Sigma catalog no. A8592), according to the manufacturer's instructions. The reaction with 3,3′,5,5′-tetramethylbenzidine liquid substrate solution (Sigma catalog no. T0440) was stopped with 1 M sulfuric acid, and plates were read at 450 nm. Eight replicates fixed in either paraformaldehyde (plasma membrane receptors) or MeOH (total receptor) were averaged, and background was subtracted (untransfected HEK293 or OK cells fixed with paraformaldehyde or MeOH). Data were normalized to plasma membrane or total expression of FLAG-CaSR, as indicated for specific experiments.

RESULTS

[^{35}S]Cysteine Pulse-Chase Labeling of WT CaSR—To examine early events in CaSR biosynthesis, we attempted to use standard approaches to pulse-label newly synthesized receptors with [^{35}S]methionine/cysteine. CaSR has relatively few methionine residues but an abundance of cysteine residues, and experiments with the standard [^{35}S]methionine/cysteine mixtures, which are heavily weighted toward [^{35}S]methionine, resulted in poor label incorporation. Labeling with [^{35}S]cysteine, however, yields high and reproducible incorporation into nascent CaSR. Fig. 1*A* illustrates the results of a 60-min pulse with [^{35}S]cysteine in HEK293 cells transiently transfected with FLAG-CaSR (36 h) and then treated with DMSO or 10 μM MG132 overnight and during the cysteine/methionine starvation period and [^{35}S]cysteine pulse. Lysates were subjected to immunoprecipitation (IP) with monoclonal anti-FLAG plus anti-GAPDH antibodies (for normalization), run on 4–15% SDS-polyacrylamide gels, and blotted to nitrocellulose membrane, followed by sequential development of the ^{35}S image and Western blot. The Western blot was cut (indicated by the *dotted line*) and probed with polyclonal anti-CaSR LRG (*top*) and anti-GAPDH antibodies (*bottom*), as described under "Materials and Methods." The blot was reconstructed to illustrate the ^{35}S image and Western blot (WB) for CaSR and Western blot image for GAPDH (Fig. 1*A*). Under reducing conditions, the dominant form of monomeric CaSR is ~140 kDa (Fig. 1*A*, *CaSR*>). The maturely glycosylated form is ~160 kDa. Incubation with MG132 leads to the appearance of unglycosylated CaSR at ~120 kDa (⇒), whereas incomplete reduction of disulfide bonds can lead to resolution of dimers/oligomers on Western blots (→). To confirm the identities of [^{35}S]cysteine-labeled bands, we used HEK293 cells stably expressing FLAG-CaSR to maximize the abundance of maturely glycosylated CaSR. Cells were labeled with [^{35}S]cysteine for 60 min and then chased in unlabeled cysteine plus methionine-containing medium for 24 h to facilitate maturation of [^{35}S]CaSR (Fig. 1*B*). Lysates were immunoprecipitated with anti-FLAG antibody and eluted with FLAG peptide. Eluates were incubated overnight at 37 °C without an addition (Fig. 1*B*, *CONTROL*) or with endoglycosidase H (*EndoH*) or peptide:*N*-glycosidase F (*PNGaseF*). Samples were run on 4–15% gels and blotted as described for Fig. 1*A*. Both the ^{35}S image and Western blot (probed with anti-CaSR LRG antibody) illustrate that the 140 kDa band is sensitive, whereas the 160 kDa band is insensitive to endoglycosidase H. In contrast,

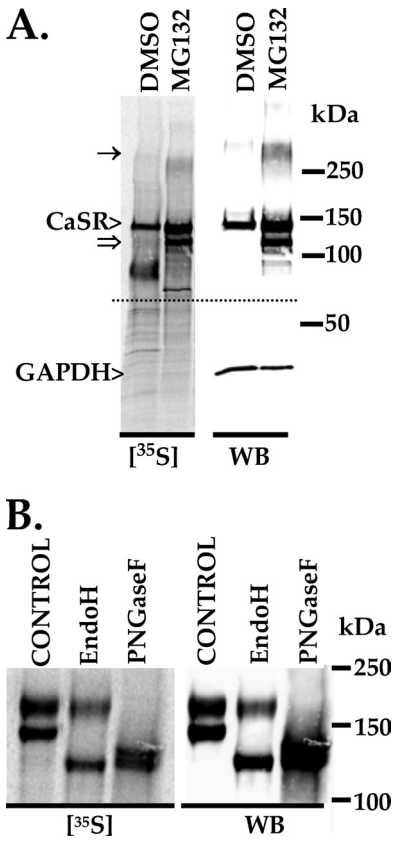

FIGURE 1. **[^{35}S]cysteine labeling of CaSR.** *A*, HEK293 cells transiently transfected with FLAG-CaSR (36 h) were incubated overnight with MG132 (10 μM) or DMSO prior to labeling. Cells were starved and labeled with [^{35}S]cysteine for 60 min, lysed, immunoprecipitated with anti-FLAG antibody, and Western blotted as described under "Materials and Methods." [^{35}S]Cysteine-labeled proteins were detected on an Amersham Biosciences Storm 840 Imager (*labeled* [^{35}S]). The same blot (*labeled WB*) was also probed with anti-CaSR (*top*) and anti-GAPDH (*bottom*) antibodies (separation marked by a *dotted line*). The locations of monomeric CaSR (*CaSR*>) and GAPDH (*GAPDH*>), the dimeric form of CaSR (→), and the deglycosylated form of CaSR (⇒) are indicated. *B*, HEK293 cells stably expressing FLAG-CaSR were labeled with [^{35}S]cysteine (60 min) and chased for 24 h to promote [^{35}S]CaSR maturation. FLAG-CaSR was immunoprecipitated with anti-FLAG Ab, eluted from protein G-agarose with FLAG peptide, and incubated (37 °C, overnight) in control buffer (*CONTROL*), endoglycosidase H (*EndoH*; Roche Applied Science), or peptide:*N*-glycosidase F (*PNGaseF*) (New England Biolabs) according to the manufacturer's instructions, followed by fractionation on SDS-polyacrylamide gels. [^{35}S]Cysteine detection and Western blotting were as in *A*.

both the 140 and 160 kDa bands were reduced to the unglycosylated form (120 kDa) by treatment with peptide:*N*-glycosidase F. The results of Fig. 1 demonstrate that CaSR can be pulse-labeled with [^{35}S]cysteine and appears in the ER as the 140-kDa form, which contains core glycosylation sensitive to endoglycosidase H. CaSR is therefore cotranslationally subjected to quality control surveillance because acute block of the proteasome with MG132 results in an increase in net [^{35}S]cysteine incorporation and appearance of the unglycosylated 120-kDa form. The experiment illustrated in Fig. 1*B* was performed in cells stably expressing CaSR, with a significant proportion of total receptors in the mature form (Fig. 1*B*, Western blot (*right*)). Despite this, less than 50% of [^{35}S]CaSR was processed to the endoglycosidase H-insensitive, peptide:*N*-glycosidase F-sensitive 160-kDa form after 24 h of chase (Fig. 1*B*, ^{35}S image (*left*)).

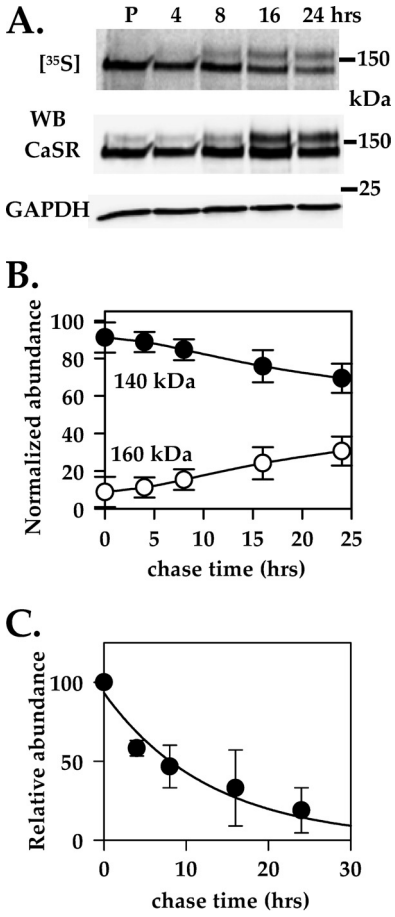

FIGURE 2. **[^{35}S]Cysteine pulse-chase of FLAG-CaSR reveals slow and incomplete maturation.** *A*, HEK293 cells transiently transfected with FLAG-CaSR for 24 h were labeled for 60 min with [^{35}S]cysteine and chased for various times prior to processing as described under "Materials and Methods." Both the ^{35}S image and WB for CaSR of a representative blot as well as the GAPDH portion of the WB are shown. *B*, quantitation of the maturation of transiently transfected FLAG-CaSR from 11 independent experiments as illustrated in *A*. Immature (140-kDa) and mature (160-kDa) CaSR at each time point were quantified with ImageQuant software (Amersham Biosciences) and plotted as normalized abundance = magnitude of either 140 or 160 kDa band divided by total [^{35}S]CaSR (sum of 140 plus 160 kDa bands) × 100 (mean ± S.D. (*error bars*) (n = 11)). *Black circles*, 140 kDa band; *white circles*, 160 kDa band. *C*, time course of degradation of [^{35}S]CaSR. HEK293 cells stably expressing FLAG-CaSR were subjected to a 60-min [^{35}S]cysteine pulse and 24-h chase period as in *A*. Relative abundance = total [^{35}S]CaSR (sum of 140 plus 160 kDa bands) at each chase time point normalized to the total [^{35}S]CaSR label incorporated during the pulse, plotted as mean ± S.D. (n = 3). The *curve* was fitted with a simple exponential decay with a half-time of 8 h.

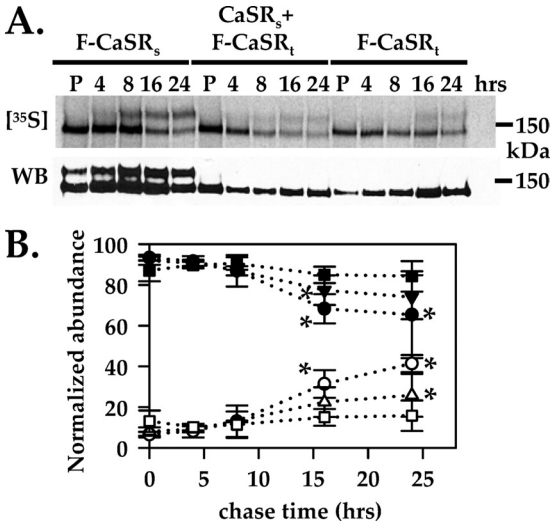

FIGURE 3. **Plasma membrane CaSR influences maturation of [^{35}S]CaSR.** *A*, HEK293 cells stably transfected with FLAG-CaSR (F-CaSR$_s$), cells stably transfected with CaSR and transiently transfected with FLAG-CaSR (CaSR$_s$ + F-CaSR$_t$), and cells transiently transfected with FLAG-CaSR (F-CaSR$_t$) were pulsed with [^{35}S]cysteine for 60 min and chased and processed as indicated under "Materials and Methods." Both [^{35}S] and WB of the same blot are shown. *B*, experiments as in *A* were quantified, and the normalized abundance of the 140 or 160 kDa bands of [^{35}S]CaSR were calculated and plotted as in Fig. 2 (mean ± S.D. (*error bars*) (n = 3)). *Black symbols*, 140 kDa CaSR; *white symbols*, 160 kDa CaSR; *square*, F-CaSR$_t$; *triangle*, CaSR + F-CaSR$_t$; *circle*, F-CaSR$_s$. Statistical significance (*, $p < 0.05$) was determined at each time point for either the 140 or 160 kDa band relative to the transient transfection condition, F-CaSR$_t$ (*squares*).

To establish the time course of [^{35}S]CaSR maturation in HEK293 cells transiently expressing FLAG-CaSR, cells were pulse-labeled with [^{35}S]cysteine for 60 min and chased in cysteine plus methionine-replete medium for varying times up to 24 h. Fig. 2*A* illustrates the ^{35}S image and Western blot (probed with anti-CaSR and anti-GAPDH antibodies) of a representative experiment. The mature 160-kDa form is first observed at 8 h of chase. Fig. 2*B* illustrates the averaged results of 11 independent pulse-chase experiments, tracking the decline in the 140-kDa (immature) form and appearance of the 160-kDa (mature) form of [^{35}S]CaSR, normalized at each time point to the sum of 140 plus 160 kDa bands, to take into account the overall decline in [^{35}S]CaSR over the 24-h period (Fig. 2*C*). Both forms are still present at 24 h and reach a steady state. In one experiment, we extended the chase period to 48 h and still observed <50% of total [^{35}S]CaSR in the mature, 160-kDa form (data not shown). These results suggest that a significant fraction of WT [^{35}S]CaSR is retained in an intracellular compartment, probably the endoplasmic reticulum based on the glycosylation state. Fig. 2*C* illustrates an estimate of the overall stability of [^{35}S]CaSR, plotting the sum of 140 plus 160 kDa [^{35}S]CaSR for three independent experiments in HEK293 cells stably expressing CaSR. Stably transfected cells were used for determination of [^{35}S]CaSR decay because total CaSR protein levels are unchanged during the chase time course. Data were fitted by a single exponential decay, with a 50% decline in [^{35}S]CaSR after 8 h.

CaSR maturation in transiently transfected cells is slow and incomplete (Fig. 2). Because stably transfected HEK293 cells exhibit a higher level of maturely glycosylated CaSR (Fig. 1*B*), we determined whether maturation of [^{35}S]CaSR was more rapid or complete in stably transfected cells. We compared three conditions: HEK293 cells stably expressing FLAG-CaSR (F-CaSR$_s$), HEK293 cells transiently transfected (24 h) with FLAG-CaSR (F-CaSR$_t$), and HEK293 cells stably expressing untagged CaSR and transiently transfected (24 h) with FLAG-CaSR (CaSR plus F-CaSR$_t$). For those conditions requiring it, cells were transiently transfected with equivalent amounts of FLAG-CaSR cDNA (6 μg) and cultured for 24 h prior to the experiments. We pulse-labeled with [^{35}S]cysteine for 60 min and chased for various times up to 24 h, followed by cell lysis and IP with anti-FLAG antibody. Results of a representative experiment are illustrated in Fig. 3*A*. The mature form of CaSR (160 kDa) was observed after 8 h. Fig. 3*B* illustrates the time

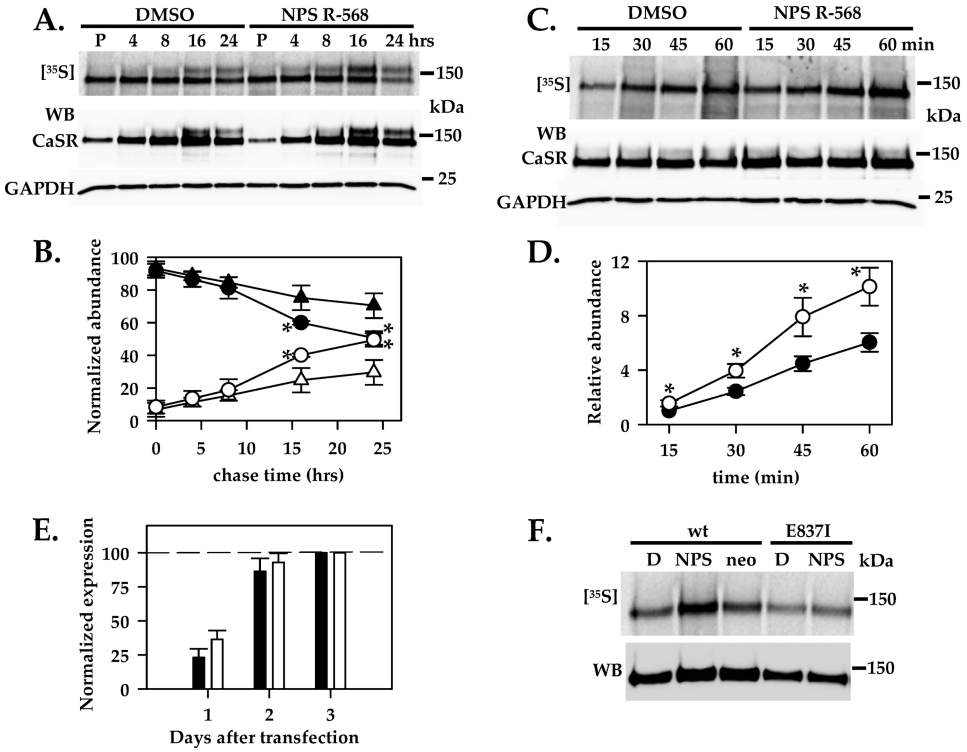

FIGURE 4. **NPS R-568 acts as a cotranslational pharmacochaperone during CaSR biosynthesis.** *A*, HEK293 cells transiently transfected with FLAG-CaSR for 24 h were exposed to NPS R-568 (10 μM) or DMSO during amino acid starvation, [^{35}S]cysteine label, and chase. Cells were harvested at the times indicated and processed as described under "Materials and Methods," and the ^{35}S image for CaSR and WB for CaSR and GAPDH of the same blot are shown. *B*, the normalized abundance of 140- and 160-kDa forms of [^{35}S]CaSR were quantified as described in Fig. 2 and plotted as mean ± S.D. (*error bars*) ($n = 3$). *Black symbols*, 140-kDa CaSR; *white symbols*, 160-kDa CaSR; *triangle*, CaSR/DMSO; *circle*, CaSR/NPS R-568. Statistical significance (*, $p < 0.05$) was determined at each time point for either the 140 or 160 band in NPS R-568 relative to DMSO. *C*, HEK293 cells transiently transfected with FLAG-CaSR for 24 h were starved, exposed to [^{35}S]cysteine for the indicated times, and immediately harvested and processed as described under "Materials and Methods." The ^{35}S image for CaSR and WB for CaSR and GAPDH of the same blot are shown. *D*, the relative abundance of [^{35}S]CaSR was determined by dividing the intensity of [^{35}S]CaSR by the intensity of GAPDH (WB). All data were then normalized to the amount of FLAG-CaSR synthesized in 15 min under control conditions and plotted as the mean ± S.E. of six independent experiments. *Black symbols*, CaSR/DMSO; *white symbols*, CaSR/NPS R-568. Statistical significance (*, $p < 0.05$) was determined at each time point for NPS R-568 condition relative to DMSO. *E*, HEK293 cells transiently transfected with FLAG-CaSR for 1, 2, or 3 days were fixed with either 4% paraformaldehyde (plasma membrane receptors; *black bars*) or MeOH (total receptors; *white bars*) and processed for ELISA as described under "Materials and Methods." Data were normalized to plasma membrane or total CaSR at 72 h (*dotted line*) and represent the average ± S.E. of nine independent experiments. *F*, HEK293 cells transfected with FLAG-CaSR (WT) or FLAG-CaSR(E837I) for 24 h were treated with DMSO (*D*), 10 μM NPS R-568 (*NPS*), or 300 μg/ml neomycin sulfate (*neo*) during amino acid starvation and the 60-min [^{35}S]cysteine label period. Cells were lysed and processed as described under "Materials and Methods." The ^{35}S image for CaSR and WB for CaSR are shown. Quantitation of the ^{35}S image showed a significant increase for FLAG-CaSR + NPS R-568 (305%) and a minor increase for FLAG-CaSR + neomycin (120%) relative to FLAG-CaSR (100%). NPS R-568 had a minimal effect on FLAG-CaSR(E837I) (129%) relative to FLAG-CaSR(E837I) (100%).

courses of [^{35}S]CaSR maturation from three independent experiments as in Fig. 3*A*. Note that the accompanying Western blot of the IP of FLAG-CaSR from the F-CaSR$_s$ line shows the presence of mature CaSR, whereas the two conditions requiring transient transfection show lower levels of FLAG-CaSR in the immature form, as expected after a 24-h transfection. Statistical analysis of each [^{35}S]CaSR form at each time point relative to the transient transfection condition (F-CaSR$_t$) indicates that the presence of stably transfected CaSR significantly increased maturation at later times (16 and 24 h; *, $p < 0.05$) but had no effect over the first 8 h. None of the conditions resulted in complete maturation of [^{35}S]FLAG-CaSR, although the extent varied, with F-CaSR$_s$ > CaSR$_s$ + F-CaSR$_t$ > F-CaSR$_t$ at 24 h. These results suggest that the steady state presence of mature CaSR significantly increases the extent of maturation of newly synthesized [^{35}S]CaSR, but neither promotes complete maturation nor significantly reduces the lag (~8 h) for the appearance of mature [^{35}S]CaSR.

Pharmacochaperone Modulation of [^{35}S]CaSR Biosynthesis and Maturation—We have previously shown that prolonged exposure (12–14 h) to the membrane-permeant allosteric agonist NPS R-568 is able to increase total and plasma membrane abundance of WT and mutant CaSRs (21, 22). Because [^{35}S]CaSR maturation is incomplete (Figs. 2*B* and 3*B*), we determined whether treatment with NPS R-568 throughout the [^{35}S]cysteine pulse-chase period could influence the rate and/or extent of [^{35}S]CaSR maturation. HEK293 cells were transfected with FLAG-CaSR (24 h) and then starved of cysteine/methionine, labeled with [^{35}S]cysteine for 60 min, and chased for up to 24 h in the continuous presence of DMSO or 10 μM NPS R-568 (Fig. 4*A*). Averaged data from three such experiments are illustrated in Fig. 4*B*. The continuous presence of NPS R-568 significantly increased the 160-kDa form and reduced the 140-kDa form of [^{35}S]CaSR at 16 and 24 h (*, $p < 0.05$). NPS R-568 does not, however, alter the lag during the first 8 h after the pulse nor induce full maturation of [^{35}S]CaSR.

Examination of the 60-min pulse suggests that the presence of NPS R-568 during the [^{35}S]cysteine labeling period may increase the amount of [^{35}S]CaSR generated (compare Fig. 4*A* pulse in DMSO *versus* NPS R-568). Averaged label incorporation during the 60-min [^{35}S]cysteine pulse in the presence of 10 μM NPS R-568 was 158 ± 21% ($p < 0.05$; $n = 5$) of that in DMSO, suggesting that membrane-permeant NPS R-568 can increase the abundance of CaSR at the earliest stages of CaSR biosynthesis. To explicitly test whether NPS R-568 acts as a cotranslational pharmacochaperone, we measured the rate of incorporation of [^{35}S]cysteine into WT CaSR at 15-min intervals over a 60-min period in the presence of DMSO or 10 μM NPS R-568, in cells transiently transfected with FLAG-CaSR (24 h). Fig. 4*C* illustrates a representative experiment, showing the ^{35}S image for CaSR and the Western blot probed for CaSR and GAPDH. The rate of [^{35}S]cysteine incorporation is significantly increased by NPS R-568. Fig. 4*D* illustrates the

combined results of six experiments. We compared the relative abundance of [^{35}S]CaSR in DMSO *versus* NPS R-568, and at all time points [^{35}S]CaSR was significantly increased by NPS R-568 ($p < 0.05$). A similar conclusion can be drawn from the rates of [^{35}S]CaSR accumulation, reflected in the slopes of the lines (*i.e.* in the presence of NPS R-568, the slope was 0.2 min^{-1}, significantly greater than in the presence of DMSO (0.11 min^{-1}) ($p < 0.05$)). Because these experiments were performed 24 h post-transfection, the effects are probably the result of NPS R-568 acting on newly synthesized receptors in the ER. The level of CaSR at the plasma membrane at 24 h is variable and is 20–25% of the level achieved at 72 h (taken as 100%), as assessed by ELISA (Fig. 4*E*). Such low levels of plasma membrane CaSR may be insufficient to fully activate signaling pathways. To further localize the site of NPS R-568 action, we compared its effects with those of neomycin, a cationic, membrane-impermeant allosteric agonist of CaSR (24). Fig. 4*F* illustrates results of a 60-min pulse with [^{35}S]cysteine, 24 h after transfection, in the presence of either DMSO (*D*), 10 μM NPS R-568 (*NPS*), or 300 μM neomycin sulfate (*neo*). As expected, NPS R-568 significantly increased [^{35}S]CaSR generation, whereas neomycin sulfate had no effect. To confirm that the effects of NPS R-568 resulted from specific binding at its allosteric site within the CaSR transmembrane domain, we compared the effects of NPS R-568 treatment on WT CaSR and the mutant CaSR(E837I) (24). Residue Glu^{837} is located at the extracellular face of helix 7 of the CaSR transmembrane domain and forms an important salt bridge with NPS R-568 to stabilize its binding (24). CaSR(E837I) is not regulated by NPS R-568 but responds normally to Ca^{2+} or phenylalanine (24). Of significance here is that synthesis of [^{35}S]CaSR(E837I) was not increased by incubation with NPS R-568 (Fig. 4*F*). The combined results of Fig. 4 suggest that NPS R-568 binds at its allosteric site within the CaSR transmembrane domain during biosynthesis (*i.e.* acts as a cotranslational pharmacochaperone) and also modestly increases maturation of CaSR to the plasma membrane at later times (16–24 h).

CaSR Mutants Encounter a Cotranslational Conformational Checkpoint—The results of Fig. 4 strongly suggest that newly synthesized [^{35}S]CaSR encounters a cotranslational pharmacochaperone-sensitive checkpoint and that the membrane-permeant allosteric agonist NPS R-568 can increase the fraction of newly synthesized CaSR that survive. We next determined whether conformational bias conferred by mutation could affect the rates of [^{35}S]cysteine incorporation into WT CaSR, the gain-of-function mutant A843E, and the loss-of-function mutant L849P. Fig. 5*A* shows a representative experiment, with both monomer and dimer zones of the blot shown (there was significant residual dimer under reducing conditions in this particular experiment). For WT and both mutants, the net abundance of receptors on the Western blot (24 h accumulation) is consistent with the relative rates of [^{35}S]cysteine incorporation determined over 1 h (*i.e.* A843E > WT CaSR > L849P). The GAPDH portion of the same blot (Fig. 5*A*) demonstrates that this is not a consequence of differential protein loading. Fig. 5*B* illustrates the normalized results of 3–5 experiments of the type in Fig. 5*A*. It is clear that the rate of [^{35}S]cysteine incorporation (slopes of lines) for the two CaSR mutants

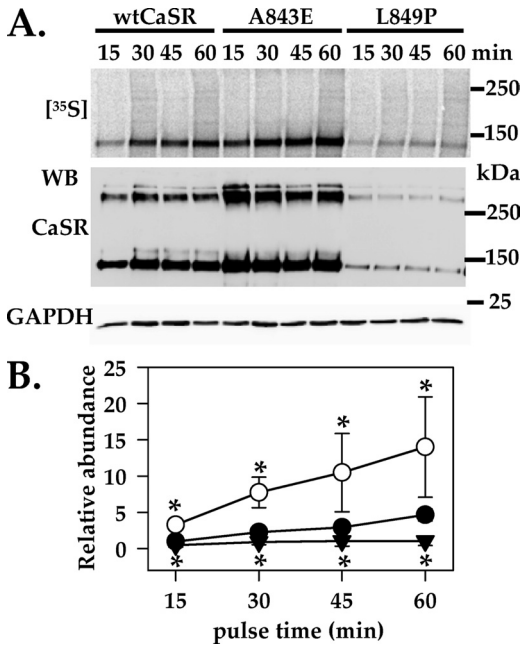

FIGURE 5. **Variable rates of CaSR mutant biosynthesis support a cotranslational conformational checkpoint.** *A*, HEK293 cells transiently transfected for 24 h with FLAG-CaSR or the mutants A843E or L849P were pulsed with [^{35}S]cysteine for the indicated times and then processed as described under "Materials and Methods." The ^{35}S image for CaSR and WB for CaSR and GAPDH of the same blot are shown. *B*, the relative abundances of WT CaSR and A843E or L849P mutants were calculated as described in the legend to Fig. 4*D* and plotted as mean ± S.D. (*error bars*) (n = 3–5). *Triangle*, CaSR(L849P); *black circles*, WT CaSR; *white circles*, CaSR(A843E). Statistical significance (*, $p < 0.05$) was determined at each time point for each mutant relative to WT CaSR. The rate of synthesis was determined by linear least squares fits to the data for WT CaSR or mutants as described in the legend to Fig. 4*D*.

differs from WT CaSR (*, $p < 0.05$ *versus* WT CaSR), varying over a 10-fold range: A843E (0.12 ± 0.02 min^{-1}) > WT CaSR (0.07 ± 0.01 min^{-1}) > L849P (0.012 ± 0.01 min^{-1}). The combined results in Figs. 4 and 5 support the existence of a cotranslational conformational checkpoint in CaSR biosynthesis that rapidly targets for destruction those receptors biased toward the inactive conformation.

Modulation of CaSR Biosynthesis by Plasma Membrane CaSR—Data in Fig. 3 suggest that the steady state presence of mature CaSR modestly increases the extent of maturation of newly synthesized receptors, although a significant fraction of receptors remain in the immature form after 24 h. We considered the possibility that signaling by plasma membrane-localized CaSR could affect the extent of maturation but that culture medium Ca^{2+} concentrations (1.1–1.8 mM) were insufficient to evoke a strong maturation signal. We therefore used the charged allosteric agonist of CaSR, neomycin sulfate (19), to potentiate CaSR activation in normal culture medium. Acute application of neomycin sulfate had no effect on [^{35}S]cysteine incorporation into CaSR during a 1-h pulse at 24 h after transfection (shown in Fig. 4*F*), when there is 20–25% of maximal plasma membrane-localized CaSR (Fig. 4*E*). We therefore initiated [^{35}S]cysteine pulse-chase experiments after 48 h of transfection, when plasma membrane-localized CaSR is nearly maximal (Fig. 4*E*). Cells were treated without or with 300 μM neomycin sulfate during the 60-min [^{35}S]cysteine pulse and the 24-h chase period. Fig. 6*A* illustrates the [^{35}S]CaSR and West-

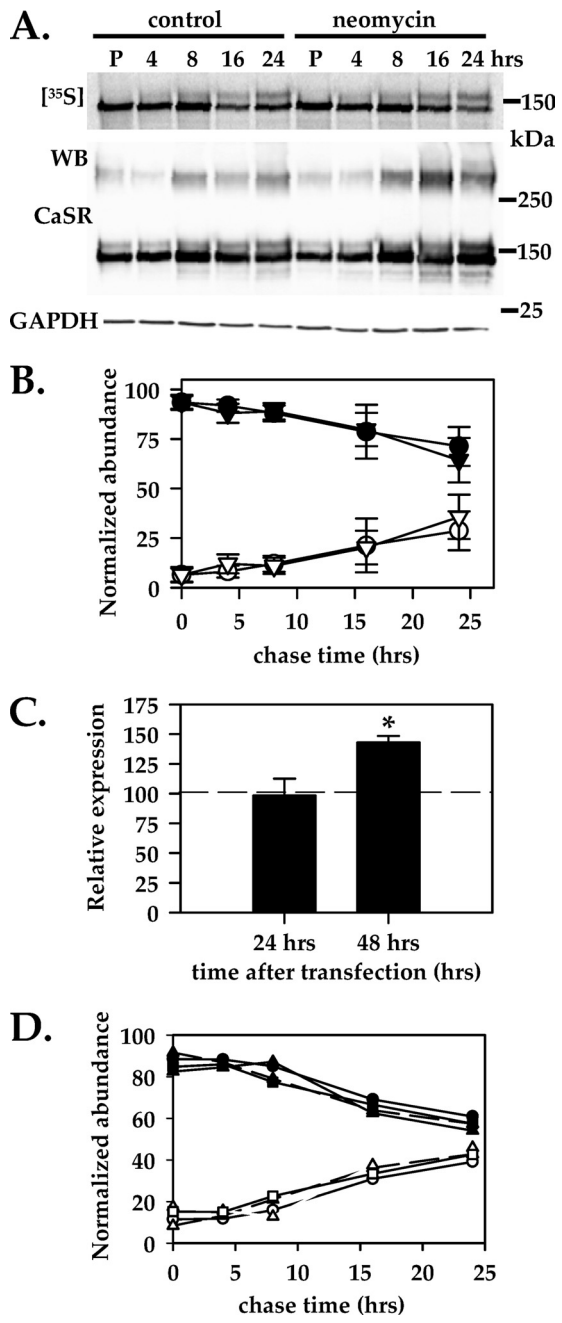

FIGURE 6. **Neomycin sulfate modulates the rate of CaSR biosynthesis but not its maturation.** *A*, HEK293 cells transiently transfected with FLAG-CaSR for 48 h were treated with 300 μg/ml neomycin sulfate during starvation, label, and chase and then harvested at the times indicated and processed as described under "Materials and Methods." The ^{35}S image for CaSR and WB for both CaSR and GAPDH of the same blot are shown. *B*, the normalized abundance of 140- and 160-kDa forms of [^{35}S]CaSR for three independent experiments were calculated as described in the legend to Fig. 2. *Black symbols*, 140 kDa; *white symbols*, 160 kDa; *circles*, control medium; *inverted triangles*, neomycin sulfate. Data are plotted as average ± S.D. (*error bars*); there were no statistically significant differences in maturation at any time point. *C*, relative expression of [^{35}S]CaSR after a 60-min [^{35}S]cysteine pulse in neomycin sulfate compared with control medium for cells transiently expressing FLAG-CaSR for either 24 or 48 h. *Bars*, [^{35}S]CaSR accumulated during the pulse in neomycin normalized to that accumulated in control medium, plotted as mean ± S.D. ($n = 3$). At 48 h, neomycin induced significantly more [^{35}S]CaSR synthesis (*, $p < 0.05$). *D*, the normalized abundance of the 140- and 160-kDa forms of [^{35}S]CaSR in variable Ca^{2+} concentration during the chase period is plotted for two independent experiments: 1) HEK293 cells stably expressing FLAG-CaSR chased with control medium (*circles*) or 5 mM Ca^{2+} DMEM (*triangles*) or 2) HEK293 cells transiently transfected with FLAG-CaSR for 48 h chased in control medium (*circles*) or 0.5 mM Ca^{2+} DMEM (*squares*). *Black symbols*, 140 kDa; *white symbols*, 160 kDa. There were no statistically significant differences in maturation at any time point.

ern blot images of a representative experiment, and Fig. 6*B* shows averaged results of three experiments. Neomycin sulfate had no significant effects on [^{35}S]CaSR maturation at any time point. The amount of [^{35}S]CaSR produced during the 60-min [^{35}S]cysteine pulse, however, was significantly increased by neomycin sulfate after 48 h of transfection (143 ± 5.5% of control, $p < 0.05$) but not after 24 h of transfection (98.5 ± 14.1, not significant) (Fig. 6*C*), suggesting that the effect is mediated by plasma membrane-localized CaSR. Both the hydrophobic (NPS R-568) and cationic (neomycin) allosteric agonists therefore increase CaSR cotranslational stability but have limited ability to facilitate CaSR maturation through the secretory pathway. The two allosteric drugs probably act via distinct mechanisms, because NPS R-568 acts cotranslationally on intracellular CaSR, whereas neomycin effects are only observed when CaSR is present at the plasma membrane.

Extracellular Ca^{2+} is an important regulator of cell function, and normal cell culture medium contains 1.1–1.3 mM Ca^{2+} plus contributions from added serum. CaSR activation by extracellular Ca^{2+} is highly cooperative (25), with EC_{50} of 3 mM for activation of PLCβ (19, 26), and thus CaSR in normal culture medium might be expected to be partially activated and/or desensitized. We considered the possibility that the intracellular pool of immature receptors may serve as a reservoir of readily releasable CaSR. We compared the effects of varying medium Ca^{2+} on maturation of CaSR by pulse-chase analysis of cells transiently or stably expressing FLAG-CaSR. Cells were pulsed with [^{35}S]cysteine for 60 min in normal medium, followed by a chase period of up to 24 h in varying medium Ca^{2+}, either normal DMEM or DMEM containing 0.5 or 5 mM Ca^{2+}. Results of individual experiments are plotted in Fig. 6*D*. Neither low nor high Ca^{2+} medium altered the basic features of [^{35}S]CaSR maturation, suggesting that the orthosteric agonist Ca^{2+} is not the prime regulator of CaSR maturation to the plasma membrane.

The CaSR CT Dictates CaSR Maturation Rate—[^{35}S]Cysteine pulse-chase analysis of CaSR biosynthesis suggests slow and incomplete maturation. Both allosteric modulators, such as neomycin or NPS R-568 and the orthosteric agonist Ca^{2+} have a limited ability to enhance the [^{35}S]CaSR maturation rate and/or extent. We therefore considered the possibility that slow maturation (*i.e.* ER retention) is a physiological requirement for normal CaSR function. Many membrane proteins contain retention, targeting, and trafficking sequences within their CTs. The CaSR CT is large (215 residues) and unique, and we tested whether it contributed to the significant intracellular retention of CaSR. We first compared WT CaSR-EGFP (chimera of full-length CaSR linked at the extreme carboxyl terminus to EGFP) with the CT chimera CaSR/mGluR1α-EGFP, containing WT CaSR sequence through CT residue 869 and rat mGuR1α residues 849–1194 followed by EGFP. Fig. 7*A* illustrates results of a 60-min [^{35}S]cysteine pulse followed by a 24-h chase period, and Fig. 7*B* illustrates the averaged results of three independent experiments. The carboxyl-terminal chimera

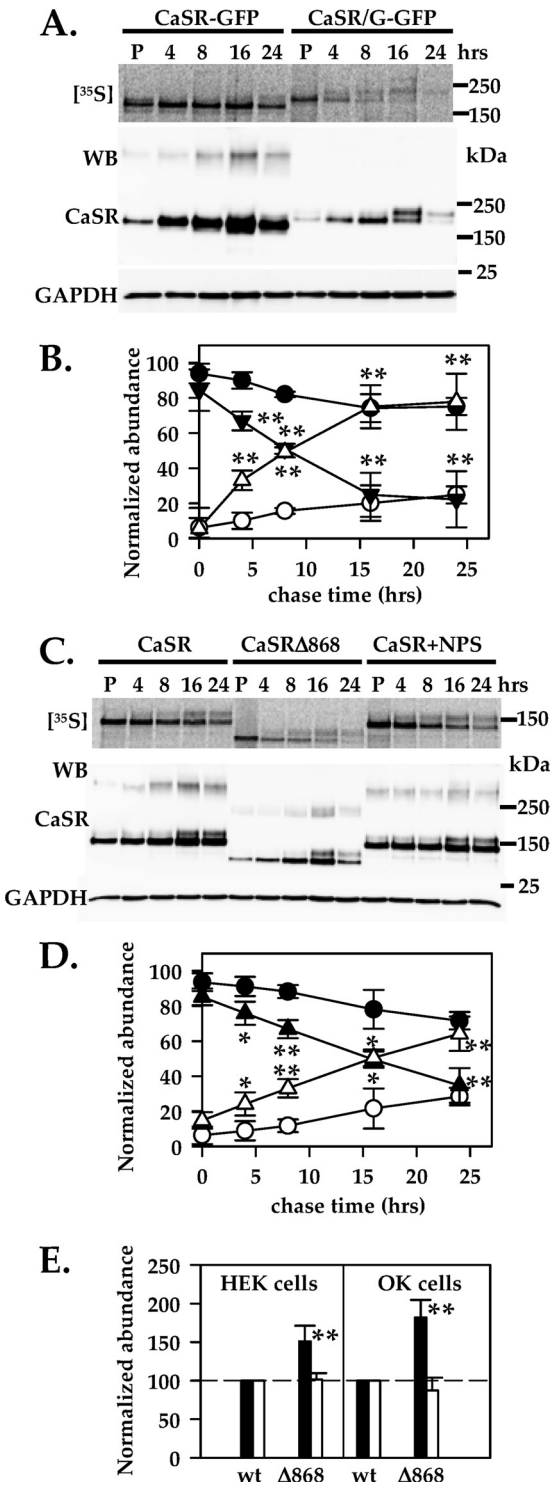

FIGURE 7. **The CaSR CT dictates the CaSR maturation rate.** *A*, HEK293 cells transiently transfected for 24 h with either FLAG-CaSR-EGFP or FLAG-CaSR/G-EGFP were [^{35}S]cysteine pulse-labeled for 60 min and chased for the times indicated, and samples were processed as described under "Materials and Methods." The ^{35}S image for CaSR and WB for both CaSR and GAPDH of the same blot are shown. *B*, the normalized abundances of immature CaSR-EGFP (*black circles*) or CaSR/G-EGFP (*black triangles*) and mature CaSR (*white circles*) or CaSR/G-EGFP (*white triangles*) were quantified as described and plotted as mean ± S.D. (*error bars*) ($n = 3$). Statistical significance ($p < 0.05$ (*) or $p < 0.005$ (**)) was determined at each time point relative to CaSR-EGFP. *C*, HEK293 cells were transiently transfected for 24-h FLAG-CaSR or FLAG-CaSRΔ868, pulsed with [^{35}S]cysteine for 60 min, and chased for the times indicated, and samples were processed as described under "Materials and Methods." NPS R-568 (10 μM) was added from starvation through chase. *D*, the normalized abundances of immature (*black symbols*) and mature (*white symbols*) FLAG-CaSR (*circles*) or CaSRΔ868 (*triangles*) were quantified as described and plotted as mean ± S.D. ($n = 3$). Statistical significance ($p < 0.05$ (*) or $p < 0.005$ (**)) was determined at each time point relative to FLAG-CaSR. *E*, ELISA to quantify relative plasma membrane (*black bars*) or total (*white bars*) expression of full-length FLAG-CaSR or the truncation FLAG-CaSRΔ868 in HEK293 and OK cells. Cells were transfected for 48 h prior to ELISA assay as described under "Materials and Methods." Data for each cell type were normalized to WT FLAG-CaSR plasma membrane or total abundance. Statistical significance (**, $p < 0.005$) was determined relative to FLAG-CaSR plasma membrane abundance in the same cell type.

FLAG-CaSR/mGluR1α-EGFP undergoes full maturation over the 24-h period, with the crossover point (50% each 140- and 160-kDa forms) at 8 h of chase, whereas the WT FLAG-CaSR-EGFP shows the limited maturation of WT CaSR documented in earlier experiments using FLAG-CaSR. These results suggest that the resistance to maturation of [^{35}S]CaSR is defined by the CaSR CT. It is possible, however, that the mGluR1α CT contains maturation-promoting elements. We therefore compared maturation of WT CaSR with the CaSR truncation CaSRΔ868 using a 60-min [^{35}S]cysteine pulse and 24-h chase period (Fig. 7, *C* and *D*). For comparison in Fig. 7*C*, we also treated full-length FLAG-CaSR with NPS R-568, which, as expected (see Fig. 4*B*), did not elicit full maturation of WT CaSR. Both the individual experiment (Fig. 7*C*) and the averaged results of three independent experiments (Fig. 7*D*) show progressive maturation of CaSRΔ868 without a significant lag period after the end of the [^{35}S]cysteine pulse, achieving 50% maturation after 16 h. The combined results of Fig. 7, *A* and *D*, argue that determinants within the CaSR CT distal to residue 868 facilitate ER retention of a significant fraction of newly synthesized [^{35}S]CaSR. To test whether the CaSR CT retention determinants also operate in cells that express endogenous CaSR, we transiently transfected proximal tubule OK cells with either WT CaSR or CaSRΔ868 and examined plasma membrane targeting using ELISAs targeted against an extracellular epitope (FLAG) as a surrogate for maturation of glycosylation. CaSRΔ868 showed significantly higher plasma membrane localization at comparable levels of total protein expression than WT CaSR in both HEK293 and OK cells (Fig. 7*E*, *black bars*), suggesting that the determinants of retention within the CaSR CT are functional in both cell types and significantly impact plasma membrane localization of CaSR.

To isolate the region of the CaSR CT mediating ER retention, we generated and transiently expressed a range of CaSR CT truncations (in the same FLAG-CaSR background), followed by anti-FLAG IP and Western blotting. Fig. 8*A* illustrates a representative Western blot. Progressive truncation of the CaSR CT not only affects maturation but also affects CaSR stability, and Fig. 8*A* therefore illustrates two different exposures of the same blot to permit accurate quantitation of mature and immature bands of monomeric CaSR. Fig. 8*B* illustrates the averaged results of four independent transfections using a wider range of truncations. Truncations shorter than CaSRΔ898 show a significant increase in maturely glycosylated CaSR, indicating that residues critical to ER retention lie between CaSRΔ868 and CaSRΔ898. This region contains an extended arginine-rich motif as well as numerous phosphorylation sites that may serve as protein interaction sites for regulated ER retention.

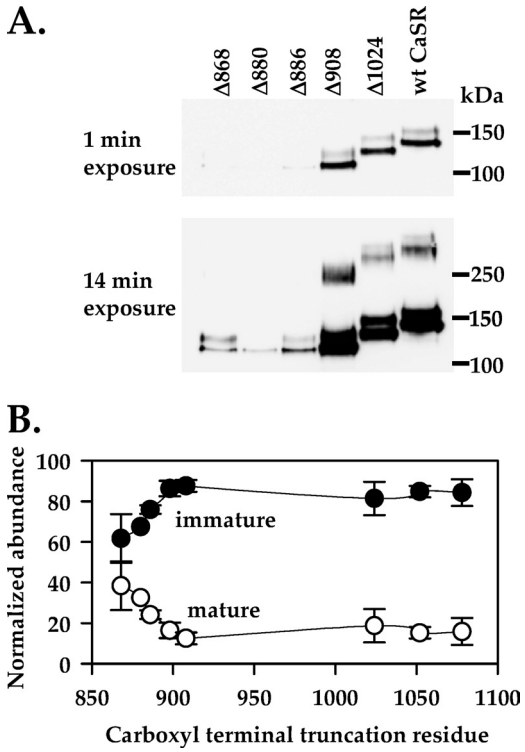

FIGURE 8. **Residues between Thr^{868} and Arg^{898} control ER retention of CaSR.** *A*, HEK293 cells were transiently transfected with 1 μg of cDNA (6-well plates) for 48 h with FLAG-CaSR or various CT truncations (CaSRΔ868, CaSRΔ880,, CaSRΔ886, CaSRΔ898, CaSRΔ908, or CaSRΔ1024), followed by cell lysis, IP with anti-FLAG antibody, and Western blotting. Blots were probed with anti-CaSR antibody, and the interval image capture mode of the FUJIFILM LAS-4000mini luminescent analyzer was used to capture 15 images at 1-min intervals. Images that were optimal for individual truncations were used for quantitation of the immature and mature monomeric forms of CaSR (which varied in mass, depending upon the degree of truncation). *B*, plot of the fraction of total CaSR in mature (*filled circles*) or immature (*open circles*) forms for WT FLAG-CaSR and truncations (CaSRΔ868, CaSRΔ880, CaSRΔ886, CaSRΔ898, CaSRΔ908, CaSRΔ1024, and CaSRΔ1052). Data were calculated as the percentage of total CaSR protein for each truncation (WT CaSR has 1078 residues). *Error bars*, S.D.

DISCUSSION

In this report, we describe the general features of CaSR biosynthesis using [^{35}S]cysteine pulse-chase methods modified to facilitate sufficient label incorporation into nascent CaSR. Several features of [^{35}S]CaSR synthesis and maturation are notably distinct from results obtained for other GPCRs, including opioid (4, 27), vasopressin (10, 28), bradykinin (29), and luteinizing hormone (30, 31) receptors. [^{35}S]CaSR is stable in the ER form (~140 kDa), and maturation to the endoglycosidase H-resistant form (~160 kDa) is generally observed 16 h after the [^{35}S]cysteine pulse. Once initiated, maturation does not go to completion but rather reaches a ratio of immature/mature forms of ≤50% for times up to 48 h. These properties are in sharp contrast to the generally immediate and rapid maturation of many newly synthesized GPCRs (27–31). It is unlikely that this large store of immature [^{35}S]CaSR represents misfolded protein awaiting degradation because ER-associated degradation is rapid (*e.g.* δ-opioid (10) and vasopressin V1b/V3 (28) receptors undergo either maturation or degradation within 4 h of synthesis). A trivial explanation for the current results is that heterologous expression of CaSR limits maturation by saturating the secretory pathway and/or as a result of the absence of cell type-specific chaperones. Two factors argue against this explanation. First, the CT chimera CaSR/mGluR1α and the CaSRΔ868 truncation undergo maturation without a lag, suggesting a specific retention mechanism. Second and more compelling is the documented presence of intracellular CaSR in a variety of cell types having endogenous expression, including keratinocytes (32, 33), where an intracellular role for CaSR has been suggested (34), kidney cells (35, 36), neurons (37), and glia (38). Enhanced plasma membrane targeting is observed for the truncation mutant CaSRΔ868 in HEK 293 cells and OK cells (opossum kidney proximal tubule cells, which express endogenous CaSR (39)), suggesting common mechanisms mediating intracellular retention of full-length CaSR.

Given that intracellular CaSR is a physiologically relevant form of the receptor, there are two potentially non-exclusive roles for the large, stable intracellular population of immature [^{35}S]CaSR. Mobilization of nascent intracellular CaSR may allow more rapid alterations in plasma membrane CaSR levels in response to cellular signaling than regulation at the transcriptional or even translational levels. Cells are chronically exposed to extracellular Ca^{2+}, and a stable intracellular pool of CaSR may represent an adaptive mechanism for sensing dynamic changes in extracellular Ca^{2+} in the face of chronic desensitization. The inability of either low (0.5 mM) or elevated (5 mM) Ca^{2+} to facilitate maturation of [^{35}S]CaSR argues against this possibility, although mobilization of CaSR may result from non-CaSR signaling. A second possibility is that intracellular CaSR may subserve distinct cellular signaling functions from that of plasma membrane CaSR, as has been demonstrated for the related Family C GPCRs, mGluR1 and mGluR5 (40–42), and Family A GPCRs, including α1 adrenergic (43), estrogen-sensitive GPR30 (44), and apelin, angiotensin AT_1, and bradykinin B_2 (45) receptors. CaSR fulfills the criteria for a GPCR with the potential for intracellular signaling (*i.e.* CaSR is stably expressed within these intracellular compartments, and it has access to its agonist, Ca^{2+}, which is concentrated within the lumen of the ER, Golgi, and nuclear envelope compartments). Further, the ER lumen contains not only Ca^{2+} but glutathione, which is an allosteric activator of CaSR (46). The present data also argue that active mechanisms are invoked to retain CaSR at significant levels within the ER. The maturation profiles of both the CaSR/mGluR1α chimera and CaSRΔ868 suggest that the CaSR CT distal to residue 868 actively participates in ER retention. Fine mapping of the maturation of CaSR truncations suggests that the interactions mediating ER retention are localized between Thr^{868} and Arg^{898} of the proximal CT. Numerous studies have characterized CaSR CT truncations (*e.g.* see Refs. 47–49), identifying roles for the proximal CT in signaling and plasma membrane targeting. The current work identifies a novel contribution of the proximal CT to ER retention. Despite the large and unique features of the CaSR CT, few interacting proteins have been identified, probably because traditional yeast two-hybrid screening approaches are not optimized for identification of protein interactions regulated by phosphorylation. The proximal CaSR CT distal to residue 868 is rich in potential phosphorylation sites for protein kinases C and A as well as casein kinases

I and II, Akt, and GSK3β (NetPhos 2.01), suggesting that protein interactions with the CaSR CT may be differentially regulated by cellular signaling. ER luminal Ca^{2+} and/or glutathione levels vary as a function of cellular signaling (50, 51) and redox status (52, 53), and ER-retained CaSR may therefore play a physiological role in integrating these diverse and dynamic signals. Careful dissection of the properties of plasma membrane *versus* intracellular CaSR-mediated signaling will be required to validate this hypothesis.

CaSR is regulated by a variety of endogenous and pharmacological allosteric modulators, including amino acids and glutathione, polyamines, and polycationic antibiotics, targeted to site(s) on the ECD, and several classes of allosteric agonists and antagonists targeted to site(s) within the heptahelical domain (reviewed in Ref. 19). We have previously shown that NPS R-568 can rescue both WT CaSR and some loss-of-function mutants identified in familial hypocalciuric hypercalcemia/neonatal severe primary hyperparathyroidism patients, increasing both total and plasma membrane-targeted levels of receptor protein and function (21, 22). Allosteric agonists may have similar effects *in vivo* because uremic rats treated with cinacalcet (54) as well as first/second generation allosteric agonists (calcimimetics) NPS R-568 (55), Amgen R-568 (56, 57), or AMG-641 (58) show reduced parathyroid gland hyperplasia, vascular calcification, and remodeling as a result of both enhanced activation and expression of CaSR in relevant tissues (54–58). The current results explicitly define the mechanism of NPS R-568 action as cotranslational stabilization of newly synthesized CaSR. Results suggest that CaSR navigates all generic (glycosylation, disulfide bond shuffling) and specific (helix packing, conformational assessment) quality control checkpoints cotranslationally, and the rate of appearance of [^{35}S]CaSR can be taken as a measure of the relative stability conferred by ambient conditions in the ER. Results with NPS R-568 on WT CaSR were recapitulated with CaSR mutations, with the rate of [^{35}S]cysteine incorporation of the representative gain-of-function mutant A843E > WT CaSR > the loss-of-function mutant L849P. Targeting of misfolded receptors to the ERAD pathway occurs cotranslationally because the presence of MG132 during the [^{35}S]cysteine labeling period induces the appearance of the unglycosylated form of the receptor. Interestingly, the continued presence of NPS R-568 during the chase period, although increasing net CaSR protein, did not eliminate the lag to initiation of maturation of [^{35}S]CaSR. Overall, these results suggest that NPS R-568 acts cotranslationally to stabilize nascent [^{35}S]CaSR but is not the dominant regulator of CaSR maturation. This is in contrast to the pharmacochaperone effects on rescue of vasopressin and gonadotrophin-releasing hormone receptors, where exposure of cells to pharmacochaperones after biosynthesis is able to rescue misfolded receptors to the plasma membrane (9, 59, 60).

The conformational checkpoint may be a unique and necessary step in the biosynthesis of CaSR, which is exposed to an agonist-rich compartment during biosynthesis. Misfolded CaSRs which are not able to achieve the active conformation may be unable to participate in the protein interactions required for maturation through the secretory pathway. ER-based conformational sampling has been reported for AMPA (α-amino-3-hydroxy-5-methyl-4-isoxazolepriopionate) and kainate receptor channels, which progress through the range of normal channel gating motions in the ER prior to release to the plasma membrane (60, 61). Mutant receptors biased toward either the open or closed conformations of the agonist binding domain have significantly different ER exit rates, and optimal ER exit occurs when the channels reversibly achieve the closed cleft state normally stabilized by agonist (61). These studies are of considerable interest because the extracellular agonist binding domains of AMPA/kainate channels are homologous to the CaSR ECD (62), and similar constraints on stability and/or ER exit of CaSR may apply.

The combined results of Figs. 3 and 6 suggest a second level of allosteric modulation of CaSR cotranslational stability, resulting from activation of plasma membrane-localized, maturely glycosylated CaSR. Neomycin and related aminoglycoside antibiotics have been shown to activate CaSR signaling with potencies positively correlated with the number of cationic charges (63). In the present studies, neomycin had no effect on the rate of [^{35}S]CaSR synthesis after 24 h of transient transfection (*i.e.* at low levels of plasma membrane CaSR), in sharp contrast to the effects of the hydrophobic allosteric agonist NPS R-568. However, neomycin significantly (~50%) increased [^{35}S]CaSR when applied after 48 h of transfection, when Western blots and ELISAs indicate significant levels of maturely glycosylated plasma membrane-localized CaSR. Neomycin is therefore not a pharmacochaperone but rather activates CaSR signaling pathways. A possible candidate is the MAPK pathway, which is robustly activated by CaSR (26). Phosphorylation of ERK1/2 has been shown to lead to Mnk1 phosphorylation, leading to enhanced translation initiation (64). Further studies are required to determine whether neomycin enhances translation initiation or mediates cotranslational stabilization of nascent [^{35}S]CaSR by as yet undefined pathways, but the current results suggest that cellular CaSR abundance may be tuned by CaSR signaling.

In summary, we have characterized the early steps in CaSR biosynthesis using [^{35}S]cysteine pulse-labeling approaches. CaSR stability is regulated cotranslationally by a conformational checkpoint that targets to ERAD receptors biased toward the inactive conformation. Receptors can be stabilized by NPS R-568, a cotranslational pharmacochaperone. CaSR maturation is actively regulated by determinants in the CaSR CT, and neither the orthosteric agonist Ca^{2+} nor the allosteric agonists NPS R-568 or neomycin are able to significantly reduce the lag prior to the initiation of maturation or drive complete maturation. These results strongly suggest that a significant fraction of CaSR is actively retained in the ER and lead to the intriguing possibility that CaSR serves a unique role(s) in an as yet undefined subcompartment of the ER. The challenges now are to characterize the potentially unique contributions of intracellular CaSR to cellular physiology and to identify the protein partners mediating CaSR retention.

Acknowledgments—We thank Dr. Klaus Seuwen (Novartis Pharma, AG) for providing the original human CaSR cDNA clone and NPS R-568 and Dr. Thomas P. Segerson (Oregon Health Sciences University) for rat mGluR1α.

REFERENCES

1. Tan, C. M., Brady, A. E., Nickols, H. H., Wang, Q., and Limbird, L. E. (2004) *Annu. Rev. Pharmacol. Toxicol.* **44,** 559–609
2. Dong, C., Filipeanu, C. M., Duvernay, M. T., and Wu, G. (2007) *Biochim. Biophys. Acta* **1768,** 853–870
3. Bulenger, S., Marullo, S., and Bouvier, M. (2005) *Trends Pharmacol. Sci.* **26,** 131–137
4. Markkanen, P. M., and Petäjä-Repo, U. E. (2008) *J. Biol. Chem.* **283,** 29086–29098
5. Conn, P. M., Ulloa-Aguirre, A., Ito, J., and Janovick, J. A. (2007) *Pharmacol. Rev.* **59,** 225–250
6. Schwieger, I., Lautz, K., Krause, E., Rosenthal, W., Wiesner, B., and Hermosilla, R. (2008) *Mol. Pharmacol.* **73,** 697–708
7. Huang, Y., Niwa, J., Sobue, G., and Breitwieser, G. E. (2006) *J. Biol. Chem.* **281,** 11610–11617
8. Robben, J. H., Sze, M., Knoers, N. V., and Deen, P. M. (2007) *Am. J. Physiol. Renal Physiol.* **292,** F253–F260
9. Wüller, S., Wiesner, B., Löffler, A., Furkert, J., Krause, G., Hermosilla, R., Schaefer, M., Schülein, R., Rosenthal, W., and Oksche, A. (2004) *J. Biol. Chem.* **279,** 47254–47263
10. Petäjä-Repo, U. E., Hogue, M., Bhalla, S., Laperrière, A., Morello, J. P., and Bouvier, M. (2002) *EMBO J.* **21,** 1628–1637
11. Leskelä, T. T., Markkanen, P. M., Pietilä, E. M., Tuusa, J. T., and Petäjä-Repo, U. E. (2007) *J. Biol. Chem.* **282,** 23171–23183
12. Chen, Y., Chen, C., Wang, Y., and Liu-Chen, L. Y. (2006) *J. Pharmacol. Exp. Ther.* **319,** 765–775
13. Janovick, J. A., Brothers, S. P., Cornea, A., Bush, E., Goulet, M. T., Ashton, W. T., Sauer, D. R., Haviv, F., Greer, J., and Conn, P. M. (2007) *Mol. Cell Endocrinol.* **272,** 77–85
14. Janovick, J. A., Patny, A., Mosley, R., Goulet, M. T., Altman, M. D., Rush, T. S., 3rd, Cornea, A., and Conn, P. M. (2009) *Mol. Endocrinol.* **23,** 157–168
15. Ray, K., Clapp, P., Goldsmith, P. K., and Spiegel, A. M. (1998) *J. Biol. Chem.* **273,** 34558–34567
16. Fan, G. F., Ray, K., Zhao, X. M., Goldsmith, P. K., and Spiegel, A. M. (1998) *FEBS Lett.* **436,** 353–356
17. Ray, K., Hauschild, B. C., Steinbach, P. J., Goldsmith, P. K., Hauache, O., and Spiegel, A. M. (1999) *J. Biol. Chem.* **274,** 27642–27650
18. Jiang, Y., Minet, E., Zhang, Z., Silver, P. A., and Bai, M. (2004) *J. Biol. Chem.* **279,** 14147–14156
19. Breitwieser, G. E., Miedlich, S. U., and Zhang, M. (2004) *Cell Calcium* **35,** 209–216
20. Brown, E. M. (2007) *Subcell. Biochem.* **45,** 139–167
21. Huang, Y., and Breitwieser, G. E. (2007) *J. Biol. Chem.* **282,** 9517–9525
22. White, E., McKenna, J., Cavanaugh, A., and Breitwieser, G. E. (2009) *Mol. Endocrinol.* **23,** 1115–1123
23. Gama, L., and Breitwieser, G. E. (2002) *Methods Mol. Biol.* **182,** 77–83
24. Miedlich, S. U., Gama, L., Seuwen, K., Wolf, R. M., and Breitwieser, G. E. (2004) *J. Biol. Chem.* **279,** 7254–7263
25. Breitwieser, G. E., and Gama, L. (2001) *Am. J. Physiol. Cell Physiol.* **280,** C1412–C1421
26. Brennan, S. C., and Conigrave, A. D. (2009) *Curr. Pharm. Biotechnol.* **10,** 270–281
27. Li, J. G., Chen, C., and Liu-Chen, L. Y. (2007) *Biochemistry* **46,** 10960–10970
28. Robert, J., Auzan, C., Ventura, M. A., and Clauser, E. (2005) *J. Biol. Chem.* **280,** 42198–42206
29. Blaukat, A., Micke, P., Kalatskaya, I., Faussner, A., and Müller-Esterl, W. (2003) *Am. J. Physiol. Heart Circ. Physiol.* **284,** H1909–H1916
30. Bradbury, F. A., Kawate, N., Foster, C. M., and Menon, K. M. (1997) *J. Biol. Chem.* **272,** 5921–5926
31. Pietilä, E. M., Tuusa, J. T., Apaja, P. M., Aatsinki, J. T., Hakalahti, A. E., Rajaniemi, H. J., and Petäjä-Repo, U. E. (2005) *J. Biol. Chem.* **280,** 26622–26629
32. Tu, C. L., Chang, W., and Bikle, D. D. (2007) *J. Invest. Dermatol.* **127,** 1074–1083
33. Tu, C. L., Oda, Y., Komuves, L., and Bikle, D. D. (2004) *Cell Calcium* **35,** 265–273
34. Mauro, T. M. (2007) *J. Invest. Dermatol.* **127,** 991–992
35. Riccardi, D., Traebert, M., Ward, D. T., Kaissling, B., Biber, J., Hebert, S. C., and Murer, H. (2000) *Pflugers Arch.* **441,** 379–387
36. Riccardi, D., Hall, A. E., Chattopadhyay, N., Xu, J. Z., Brown, E. M., and Hebert, S. C. (1998) *Am. J. Physiol.* **274,** F611–F622
37. Vizard, T. N., O'Keeffe, G. W., Gutierrez, H., Kos, C. H., Riccardi, D., and Davies, A. M. (2008) *Nat. Neurosci.* **11,** 285–291
38. Chattopadhyay, N., Legradi, G., Bai, M., Kifor, O., Ye, C., Vassilev, P. M., Brown, E. M., and Lechan, R. M. (1997) *Brain Res. Dev. Brain Res.* **100,** 13–21
39. Ward, D. T., McLarnon, S. J., and Riccardi, D. (2002) *J. Am. Soc. Nephrol.* **13,** 1481–1489
40. Jong, Y. J., Kumar, V., Kingston, A. E., Romano, C., and O'Malley, K. L. (2005) *J. Biol. Chem.* **280,** 30469–30480
41. Kumar, V., Jong, Y. J., and O'Malley, K. L. (2008) *J. Biol. Chem.* **283,** 14072–14083
42. Jong, Y. J., Kumar, V., and O'Malley, K. L. (2009) *J. Biol. Chem.* **284,** 35827–35838
43. Wright, C. D., Chen, Q., Baye, N. L., Huang, Y., Healy, C. L., Kasinathan, S., and O'Connell, T. D. (2008) *Circ. Res.* **103,** 992–1000
44. Revankar, C. M., Mitchell, H. D., Field, A. S., Burai, R., Corona, C., Ramesh, C., Sklar, L. A., Arterburn, J. B., and Prossnitz, E. R. (2007) *ACS Chem. Biol.* **2,** 536–544
45. Lee, D. K., Lança, A. J., Cheng, R., Nguyen, T., Ji, X. D., Gobeil, F., Jr., Chemtob, S., George, S. R., and O'Dowd, B. F. (2004) *J. Biol. Chem.* **279,** 7901–7908
46. Wang, M., Yao, Y., Kuang, D., and Hampson, D. R. (2006) *J. Biol. Chem.* **281,** 8864–8870
47. Ray, K., Fan, G. F., Goldsmith, P. K., and Spiegel, A. M. (1997) *J. Biol. Chem.* **272,** 31355–31361
48. Gama, L., and Breitwieser, G. E. (1998) *J. Biol. Chem.* **273,** 29712–29718
49. Bai, M., Trivedi, S., and Brown, E. M. (1998) *J. Biol. Chem.* **273,** 23605–23610
50. Park, M. K., Petersen, O. H., and Tepikin, A. V. (2000) *EMBO J.* **19,** 5729–5739
51. Landolfi, B., Curci, S., Debellis, L., Pozzan, T., and Hofer, A. M. (1998) *J. Cell Biol.* **142,** 1235–1243
52. Chakravarthi, S., Jessop, C. E., and Bulleid, N. J. (2006) *EMBO Rep.* **7,** 271–275
53. Csala, M., Bánhegyi, G., and Benedetti, A. (2006) *FEBS Lett.* **580,** 2160–2165
54. Kawata, T., Nagano, N., Obi, M., Miyata, S., Koyama, C., Kobayashi, N., Wakita, S., and Wada, M. (2008) *Kidney Int.* **74,** 1270–1277
55. Mizobuchi, M., Hatamura, I., Ogata, H., Saji, F., Uda, S., Shiizaki, K., Sakaguchi, T., Negi, S., Kinugasa, E., Koshikawa, S., and Akizawa, T. (2004) *J. Am. Soc. Nephrol.* **15,** 2579–2587
56. Koleganova, N., Piecha, G., Ritz, E., Schmitt, C. P., and Gross, M. L. (2009) *Kidney Int.* **75,** 60–71
57. Piecha, G., Kokeny, G., Nakagawa, K., Koleganova, N., Geldyyev, A., Berger, I., Ritz, E., Schmitt, C. P., and Gross, M. L. (2008) *Am. J. Physiol. Renal Physiol.* **294,** F748–F757
58. Mendoza, F. J., Lopez, I., Canalejo, R., Almaden, Y., Martin, D., Aguilera-Tejero, E., and Rodriguez, M. (2009) *Am. J. Physiol. Renal Physiol.* **296,** F605–F613
59. Conn, P. M., Knollman, P. E., Brothers, S. P., and Janovick, J. A. (2006) *Mol. Endocrinol.* **20,** 3035–3041
60. Mah, S. J., Cornell, E., Mitchell, N. A., and Fleck, M. W. (2005) *J. Neurosci.* **25,** 2215–2225
61. Penn, A. C., Williams, S. R., and Greger, I. H. (2008) *EMBO J.* **27,** 3056–3068
62. Felder, C. B., Graul, R. C., Lee, A. Y., Merkle, H. P., and Sadee, W. (1999) *AAPS PharmSci.* **1,** E2
63. Katz, C. L., Butters, R. R., Chen, C. J., and Brown, E. M. (1992) *Endocrinology* **131,** 903–910
64. DeWire, S. M., Kim, J., Whalen, E. J., Ahn, S., Chen, M., and Lefkowitz, R. J. (2008) *J. Biol. Chem.* **283,** 10611–10620